Glyph-Based Visualization of Myocardial Perfusion Data and Enhancement with Contractility and Viability Information

S. Oeltze[1] and A. Hennemuth[2] and S. Glaßer[1] and C. Kühnel[2] and B. Preim[1]

[1]Department of Simulation and Graphics, University of Magdeburg, Germany
[2]MeVis Research GmbH, Bremen, Germany

Abstract

Perfusion data characterize the regional blood flow in human tissue. In the diagnosis of the Coronary Heart Disease, they are acquired to detect hypoperfused regions of the myocardium (heart muscle) at an early stage or to evaluate the hemodynamical relevance of a known pathologic vessel narrowing. For each voxel in the data, a time-intensity curve describes the enhancement of a contrast agent. Parameters derived from these curves characterize the regional perfusion and have to be integrated for diagnosis. The diagnostic evaluation of this multi-field data is challenging and time-consuming due to its complexity. We tackle this problem by developing a glyph-based integrated visualization of perfusion parameters in 3D-space with the patient-individual ventricular anatomy as context information.
Besides the assessment of myocardial perfusion, current cardiac imaging technology allows for the investigation of myocardial contractility as well as for the detection of non-viable tissue. The combined inspection of these data supports diagnosis finding and therapy planning by allowing for the discrimination of healthy, hypoperfused and non-viable tissue as well as between non-viable and temporarily inactive tissue. To facilitate such an inspection, we apply registration methods that cope with differences in orientation and coverage between these three datasets. We enhance the glyph-based visualization of perfusion parameters by integrating parameters describing the myocardial contractility and viability.

Categories and Subject Descriptors (according to ACM CCS): J.3 [Life and Medical Sciences]: Health

1. Introduction

A severe stenosis (an abnormal vessel narrowing) or occlusion of one or more coronary arteries is referred to as Coronary Heart Disease (CHD). The consequences of CHD head the list of causes of death in industrial countries. Angina pectoris, cardiac arrhythmia and heart attack may result from the restricted blood supply of the myocardium (heart muscle). At an early stage, the CHD is characterized by a perfusion defect. Hence, the detection and localization of such a defect as well as the assessment of its severity are relevant. Major diagnostic tasks are to evaluate whether the patient suffers from CHD, to evaluate the severity of the disease and to assess the vascular supply of less perfused tissue [HSB06]. We focus on Magnetic Resonance Imaging (MRI) which offers an especially attractive alternative to image modalities from nuclear medicine since measures of myocardial perfusion, contractility and viability can be integrated in a single scanning protocol.

In perfusion imaging, the distribution of a contrast agent (CA) is registered to assess blood flow and tissue kinetics. For each voxel, a time-intensity curve (TIC) characterizes the CA enhancement. How long it takes until the maximum amount of CA is delivered, which maximum is achieved, as well as other parameters are derived from these curves for medical diagnosis. The derived parameters represent a special instance of multi-field data, which is becoming more and more important in medicine [BBP07]. The integrated analysis of several parameters in a suspicious region is essential, since no single parameter fully describes the complex sequence of CA wash-in and wash-out. Furthermore, the reliability of an individual parameter may vary, dependent on the scanning sequence used or the type of CA and its applied dose [ASGBea01].

In informal discussions with our clinical collaborators, we learned that a visual representation of the perfusion in 3D space within the anatomical context helps to assess the global myocardial perfusion. The application of direct or indirect volume rendering techniques is not suitable due to the low number of slices that is usually acquired (3-4). Therefore, we apply glyphs for the integrated 3D display of several perfusion parameters in their anatomical context. As context information, we extract the left ventricular surface from additional cardiac data which has been acquired during the same scanning protocol. Cine data which conveys myocardial contractility as well as Late enhancement (LE) data which directly depicts non-viable tissue provide a more subtle coverage of the ventricle (10-12 slices).

Besides providing anatomical context information, the integration of these additional data supports diagnosis finding and therapy planning by allowing for the discrimination of healthy, hypoperfused and non-viable tissue as well as between non-viable and hypoperfused, temporarily inactive tissue. The latter may benefit from a so-called *revascularization therapy*. To facilitate a joint inspection of perfusion, cine and LE data, we apply registration methods that cope with differences in orientation and coverage between these three datasets. We then derive parameters describing myocardial contractility and viability from the additional data and enhance the glyph-based visualization of perfusion parameters by integrating them.

2. Medical Background

This section gives a brief overview on perfusion diagnosis with a focus on myocardial perfusion. Furthermore, it acquaints the reader with the basics of contractility and viability assessment by means of cine and LE imaging. For detailed information on all three imaging techniques, with respect to the acquisition as well as the diagnostically relevant parameters, see [SRFN06]. Due to the broad variety of imaging sequences and scanning devices, we omit the listing of typical dataset characteristics. Instead, we provide a general description of the data and present the precise characteristics of our case studies in Subsec. 4.1.

2.1. Perfusion Diagnosis

In perfusion imaging, a CA is injected intravenously and its distribution is measured by a repeated acquisition of subsequent images covering the volume of interest. The CA provides signal changes in the acquired 4D data (3D+time). It circulates through the body in several passages until it gets completely excreted. Normally, the first CA passage, which shows the most significant signal changes, is evaluated. In case of a perfusion defect, the corresponding region exhibits an abnormal change in signal intensities. The spatial resolution and the Signal-to-Noise ratio (SNR) of perfusion data are lower than those of static data. Computed Tomography (CT), Positron Emission Tomography (PET),
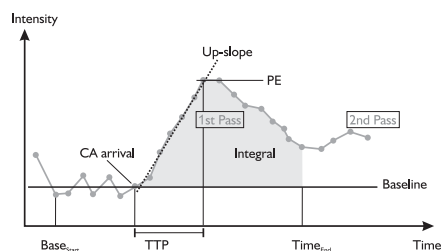

Figure 1: *A typical time-intensity curve for healthy tissue in myocardial perfusion with a significant first pass and an alleviated second pass of contrast agent traversal annotated with the essential parameters to evaluate the first pass.*

Single Photon Emission Computed Tomography (SPECT) and MRI data are employed for perfusion imaging. The data acquisition is typically accomplished as suggested by the American Heart Association (AHA) in 3-4 cardiac short-axis planes [CWDea02]. The planes are acquired during breath-hold and electrocardiogram (ECG)-triggered over several consecutive heart beats. Since only 3-4 slices are acquired, with an inter-slice distance greater than twice the slice thickness, there is a considerable acquisition gap, i.e. a poor ventricular coverage.

Perfusion Parameters. For the diagnosis, regions of interest in healthy and suspicious tissue are defined, and TICs—averaged over all voxels in the selected region—are analyzed. Depending on the application area, different sets of parameters, derived from the curves, are relevant. Fig. 1 illustrates the parameters that have been approved in cardiac perfusion diagnosis, e.g., in [ASGBea01], and [PGYea01]. For a detailed discussion on all parameters, their derivation and diagnostic meaning, see [ODHea07]. Briefly, the diagnostically relevant parameters in cardiac perfusion are:

- *Peak Enhancement (PE)*. The maximum value normalized by subtracting the *Baseline*. The *PE* separates the first CA passage (1*st pass*) into a phase of CA *wash-in* followed by the CA *wash-out*.
- *Time To Peak (TTP)*. The time until *PE* occurs, normalized by subtracting *CA arrival* time.
- *Integral*. For the duration of the first pass, the area between the curve and the *Baseline*—the approximated integral—is computed.
- *Up-slope*. The steepness of the curve during wash-in.

Bull's Eye Plot. Due to the low SNR of perfusion data, often a segment-wise analysis of averaged perfusion parameters is preferred. The prevailing way of presenting the averaged information is the so-called *Bull's-Eye Plot* (BEP). To construct the BEP, the myocardium is divided into 17 segments, according to suggestions of the AHA (AHA model) [CWDea02]. In Fig. 2 (a), the division into six segments is illustrated for the basal slice. The mid-cavity is also divided into six and the apical slice into four segments. The
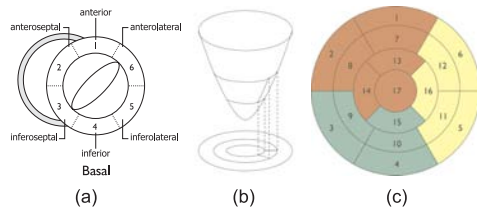
Figure 2: *AHA-conform division of the myocardium in the basal slice* `(a)`*. By fictitiously projecting all segments onto a plane* `(b)`*, the Bull's Eye Plot is generated* `(c)`*. Different colors indicate a different supplying coronary main branch.*

apex forms a segment itself. The BEP is then constructed by fictitiously projecting all segments onto a plane (Fig. 2 (b)) providing a representation of the ring-shaped myocardium over all image slices (Fig. 2 (c)). The correspondence between myocardial and BEP segments is established via polar coordinates. The BEP segments are usually colored according to the averaged perfusion parameter of the corresponding myocardial segment. In Fig. 2 (c), different colors indicate a different supplying coronary main branch. Due to the rough division according to the AHA model, the precise extension of, e.g., an ischemic region, may remain uncertain. In this case, a more subtle, user-defined division may be preferred. Besides being used in perfusion diagnosis, the BEP is also applied for communicating parameter values in contractility and viability diagnosis.

2.2. Myocardial Contractility and Viability Diagnosis

In cardiac MR imaging, measures of myocardial perfusion, contractility (also referred to as *function*) and viability can be integrated in a single scanning protocol. The combined inspection of these data supports diagnosis finding and therapy planning. Applying the LE data, the myocardial tissue can be classified into non-viable and viable. Viable tissue can be further differentiated with the help of the contractility information and the perfusion parameters. Normally perfused myocardium with a dysfunction that is persistent for max. 2 weeks after acute ischemia is referred to as *stunned myocardium*. Hypoperfused tissue which exhibits a normal function and *hibernating myocardium* which shows hypoperfusion and a decreased function may both benefit from a revascularization therapy where the responsible narrowed part of the coronaries is widened.

Contractility. The response of the myocardium to a decreased blood supply (*ischemia*) occurs in a determined order referred to as ischemic cascade. The cascade starts with a diminished perfusion in the affected myocardium which results in a hampered relaxation process and subsequent decrease of contractility measured by reduced *myocardial thickening* and inward motion. In literature, the myocardial thickening is mostly referred to as *wall thickening* (WT).

To evaluate WT and other, global functional parameters, e.g., the ejection fraction or cardiac mass, a 4D dataset is acquired during breath-hold covering one heart cycle from end-diastole (ED = end of myocardial relaxation) to end-systole (ES = end of myocardial contraction). In contrast to perfusion data, where the heart is imaged always at the same timepoint during the cardiac cycle, cine data shows the beating heart. Typically, cine data provides a higher spatial ventricular coverage than the perfusion data. A common approach for assessing the local WT is to first, determine the end-diastolic and end-systolic timepoint and then, to measure WT as the local percentage increase in wall thickness from ED to ES [SBDea86]. The resulting WT is often presented segment-wise in a BEP.

Viability. When the blood supply of the myocardium is massively hampered or entirely absent for a period of 20 to 30 minutes, myocardial tissue is irreversibly damaged (non-viable) and eventually an infarct occurs. The affected tissue (infarction scar) can directly be visualized by means of LE imaging. Here, approximately 10-15 minutes after the CA injection for perfusion imaging, an additional 3D dataset is acquired during ED applying an inversion recovery TurboFlash sequence. The higher distribution volume for the CA in infarcted tissue leads to an increase of signal intensity in the image slices [ASHea99]. Typically, the slices are acquired at the same imaging planes as the cine data. The most important viability parameter, besides the existence and location of infarcted tissue, is its *transmurality*. The transmurality (TM) locally describes the penetration degree of myocardium with infarction from the endocardium (inner ventricular wall) to the epicardium (outer ventricular wall). It is often computed segment-wise and presented in a BEP. According to Choi et al. [CKGea01], TM facilitates a prediction of the long-term improvement in contractility.

3. Prior and Related Work

This section describes prior and related work on the application of glyph-based techniques as well as on visualization methods for supporting CHD diagnosis.

3.1. Glyph-based Medical Visualization

In [RP08], a glyph taxonomy and usage guidelines for glyph-based medical visualization are presented. In addition, existing glyph-based visualizations are reviewed with respect to this taxonomy. Thereby, the focus is on the application of glyphs in diffusion tensor imaging and in cardiac diagnosis. In this subsection, we extend the latter part. Choi et al. apply glyphs for visualizing ventricular function parameters obtained by fitting a heart model throughout the cardiac cycle in cine data [CLYK03]. In [WLY04], color-coded ellipsoids are employed for visualizing the myocardial strain based on a model and finite element simulations. *Color-icons* were applied in [OGHea06] for the slice-based

integrated visualization of up to four myocardial perfusion parameters. In [POHea07], the glyph-based integrated visualization of perfusion, contractility and viability parameters has been presented. Simple 3D glyph shapes are placed either voxel- or segment-wise (according to the AHA model) in the context of the left ventricular surface and the infarction scar. Ropinski et al. apply superquadrics for a hybrid visualization of PET and CT data [RMSSea07]. They put special emphasis on avoiding visual clutter by means of dedicated placement strategies. The integrated glyph-based 2D visualization of multiple perfusion parameters is presented by Oeltze et al. [OMP08] with a focus on an easy to learn glyph coding of TIC shape.

3.2. Visualization for CHD Diagnosis

The cinematic depiction of gray scale images is the simplest way of investigating 4D cardiac data. It is helpful for the assessment of enhancement patterns in perfusion data and for evaluating the left ventricular wall motion in cine data. Commercial workstations (*Argus Dynamic Signal*, SIEMENS) and perfusion analysis software packages (*CMRtools*, Imperial College; *QMassMR*, Medis) allow the definition of Regions of Interest or a division of the myocardium according to the AHA model, an analysis of the corresponding averaged TICs and a BEP visualization. The BEP visualization is also applied for the segment-wise analysis of contractility and viability information. A pixel-wise examination by means of color-coded parameter maps reveals the regional distribution of selected perfusion parameters [PGYea01]. However, the analysis of parameter combinations in a tiled visualization requires a mental integration of suspicious regions. Hence, multiparameter visualizations, integrating several perfusion parameters in one image, were introduced in [OGHea06]. Multivariate color scales, color icons and colored height fields were discussed. In order to simplify a mental integration of rest and stress perfusion in one area, a refined BEP was introduced in [OGHea06]. Recently, data analysis techniques and information visualization techniques have been combined in to explore the space of perfusion parameters [ODHea07].

Integrated Visualization of Different Scans. Breeuwer et al. suggest a combination of LE and perfusion data supporting the differentiation between hypoperfused and infarcted tissue [BPNea03]. For that purpose, the infarction area is segmented and superimposed on the BEP which presents the perfusion analysis results. The automatic detection of hibernating myocardium is presented in [NHBR04]. First, the transmurality of the infarcted tissue as well as the wall thickening are computed and second, they are competitively weighted. The result is then color-coded on the left ventricular surface. Oeltze et al. support the joint inspection of MR perfusion and CT Coronary Angiography data by establishing a bi-directional link between the BEP and a 3D view of the coronaries [OGHea06]. Picking facilities for

both, the plot and the 3D view are provided. In [SSJea06], the software assistant HeAT for the analysis of myocardial contractility after an infarction is introduced. Hennemuth et al. present registration methods for aligning perfusion and LE data, as well as visualization methods that support a joint inspection [HBKea07]. The combination of whole-heart cardiac MR, depicting ventricular and coronary morphology, and LE data has been studied by Termeer et al. [TBBea07]. They developed a volumetric extension of the BEP, preserving continuity and wall thickness, that supports a transmurality analysis. The volumetric BEP is linked to a 3D view that represents the viability information in the context of the morphologic data.

4. Image Data and Pre-processing

In this section, we describe the image data our work is based on as well as data pre-processing steps, in particular the applied registration and segmentation methods.

4.1. Image Data

This work is based on image data which has been acquired in a low-dose CA study by Dr. Frank Grothues (University hospital Magdeburg). 15 patients participated in the study which had all suffered from an infarction within one year prior to the study. The sub-images of Fig. 4 have been generated based on two representative cases, $case_1$ and $case_2$. In $case_1$, the infarction scar is located within the inferior and inferolateral wall whereas in $case_2$, it spans the anterolateral and inferolateral wall. Data acquisition was carried out on a SIEMENS TRIO (3Tesla) MR scanner. The characteristics of the corresponding datasets are:

Perfusion Data Four short-axis slices with 8 mm thickness, an in-plane-resolution of 1.875 mm x 1.875 mm, and a gap of 10 mm were imaged per heart beat using a TurboFlash (TF) sequence and ECG-triggering. The acquisition was carried out over 40 consecutive heart beats.

Cine Data The contraction sequence was acquired prior to the perfusion sequence with an inversion recovery TF sequence. 10 short-axis slices with 6 mm thickness, a gap of 4 mm and an in-plane-resolution of 1.4 mm x 1.4 mm represent one contraction cycle in 30 phases.

Late Enhancement Data 10 to 15 minutes after CA injection, the 3D LE data was acquired with the same orientation and resolution as the cine data applying a TF 3D sequence. The imaged phase corresponds to the ED in the cine data.

4.2. Image Data Pre-Processing

Patient breathing and contractile heart motion can influence the acquisition, so that an image slice at one spatial position can show the heart at different positions or in a different shape if it is acquired at different time points. Therefore,

the combined inspection of the given cardiac image data demands methods that compensate for the movement. We use the end-diastolic image of the cine data as reference image for the alignment of the perfusion, cine, and LE data.

The LE data is registered slice-wise with the reference image using rigid transformations. The transformation parameters are optimized with the so-called Simplex algorithm [NM65] and Normalized Cross Correlation as similarity measure.

The perfusion data is acquired with ECG-triggering, so that every time frame shows the same contraction phase as its temporal predecessor. However, displacement due to breathing motion frequently occurs within the image sequence. Thus, motion correction has to be performed for the whole sequence. The slices of a reference time frame, which shows CA in the bloodpool but not yet in the myocardium, are registered with the reference image of the cine data as described above. Then, the consecutive time frames are registered with their corrected predecessors as described in [HBKea07].

To analyze the spatially aligned images, the myocardium is segmented with the Live Wire algorithm by [SPP00] in all datasets. After the motion correction of the perfusion data, only one timestep needs to be segmented. The resulting contours are then propagated over time. For the cine data, the segmentation is limited to the end-diastolic and end-systolic phase. The infarction scar is segmented with the histogram analysis method proposed in [HSFea08]. The intensity distribution within the segmented myocardium is analyzed by fitting the mixture model of a Rayleigh distribution and a Gauss distribution. The determined threshold is then used to segment the myocardial regions, which exhibit late enhancement. The result of all segmentations is a binary mask.

To visualize the segmented structures in 3D, they are represented as surfaces generated by means of the Marching Cubes algorithm [LC87]. Due to the discrete nature of the data, the resulting surfaces exhibit so-called stair-case artifacts. Those artifacts hamper a reliable computation of inter-surface distances which will be applied for WT and TM computation in Sec. 6. Hence, as a pre-processing step, the surfaces are smoothed applying the λ/μ Filter [Tau95].

The perfusion parameters *PE, TTP, Integral* and *Up-slope* (Subsec. 2.1) are calculated for all myocardial voxels and stored in *parameter volumes*. Based on the binary mask of the perfusion data, myocardial properties are calculated which are needed for the glyph placement (Subsec. 5.1). For each slice s, $s \in [1, number\ of\ slices]$, the center of gravity of myocardial voxels ($COGmyo_s$) is computed. Further, the minimum, maximum and average Euclidean distances from ($COGmyo_s$) to myocardial voxels in s are determined in voxel as well as in world space.

A final pre-processing step is related to the segment-wise parameter analysis of the perfusion data (recall Sec. 2.1). It has to be repeated whenever the user switches from the AHA model to a user-defined division or changes the number of segments in the latter case. For each segment, the corresponding myocardial voxels are determined. Based on that information, the average parameter values as well as the

$COGseg_{ID}$ of the segment with the unique identification *ID* are computed. This is needed later on for modifying glyph attributes and for glyph placement, respectively. To support and improve the readability of the following sections, we summarize and add a few abbreviations:

- $BMmyo_{perf}$: Binary mask from perfusion data showing the segmented myocardium,
- $COGmyo_s$: Center of gravity of myocardial voxels the slice s in $BMmyo_{perf}$,
- $COGseg_{ID}$: Center of gravity of all myocardial voxels in $BMmyo_{perf}$ belonging to the segment labelled with *ID*,
- $SF\{lv, rv\}_{LE}$: Left (lv) and right (rv) ventricular surface from LE data,
- $SFepi_{LE}$: Epicardial surface from LE data,
- $SF\{epi, endo\}_{cine\{ED,ES\}}$: Endocardial (endo) and epicardial (epi) surface from cine data at ED and ES, respectively,
- $SFrv_{cineED}$: Right ventricular surface from cine data at ED,
- $SFscar_{LE}$: Surface of the scar from LE data.

5. Glyph-based Visualization of Myocardial Perfusion

In this section, we describe our new visualization techniques, in particular glyph placement and glyph design.

5.1. Glyph Placement and Glyph Design

The images illustrating this section (Fig. 4 (a-g)), have been generated based on $case_1$. In each image, $SFlv_{LE}$ serves as context information and is rendered semi-transparently. The lack of perceivable surface texture and object boundaries is compensated in Fig. 4 (a-c) by a superimposition of feature edges and in Fig. 4 (d-g) by a silhouette rendering. The infarction scar is rendered as a brownish surface inside the ventricle. Glyph legends illustrate the mapping of perfusion parameters to glyph attributes.

The two crucial aspects of glyph design are glyph placement and the definition of a meaningful glyph shape. Our selection of a placement strategy directly influences the range of feasible glyph shapes. If the original perfusion data exhibit a high SNR and could be reliably motion-corrected, the user may consider a voxel-wise perfusion analysis. For that purpose, a glyph is generated and centered at each voxel midpoint of the original perfusion data slices. The midpoint coordinates in 3D are computed by means of a matrix M that describes the transformation from voxel to world space. M is retrieved from the DICOM-header. Often, cardiac perfusion data exhibit a low SNR and the user will carry out a segment-wise analysis, e.g., based on the AHA model. Then, a glyph is generated for each segment and centered at $COGseg_{ID}$. To enable a more subtle division (recall Subsec. 2.1), the user may select an arbitrary number of segments per slice. The glyph placement is then updated accordingly.

Simple Glyph Shapes. In initial tests, we experimented

with simple glyph shapes, e.g. cubes and spheres. We employed two degrees of freedom, color and size. Both are modified according to the assigned parameter values and the parameters' minimum and maximum values. The real color is derived from a color look-up table (CLUT). As a default CLUT, a blue (low in oxygen) to red (oxygen rich) scale is applied which is borrowed from other systems in use in Cardiology. The maximum size of a glyph is initially restricted to the in-plane size of a voxel. An arbitrary number of coloring and scaling steps can be chosen by the user. Instead of a step-wise function, a continuous scaling can be selected.

For a voxel-wise placement, cubes delivered the best results since a cube optimally fills in the voxel area it represents. In Fig. 4 (a), *PE* and *Up-slope* are mapped to cube color and size, respectively. In the infarction zone, small bluish glyphs approve the expected perfusion defect. For illustration purposes, the glyphs have been slightly enlarged. Since their size now exceeds the in-plane size of a voxel, overlapping and z-fighting occur in a few regions.

Often, the user may wish to examine the perfusion segment-wise. In Fig. 4 (b), the myocardium has been divided according to the AHA model and a cube has been placed per segment. The segment borders are indicated by line segments that originate at $COGmyo_s$. This visualization suffers from two major problems. Due to a lack of depth information, it is difficult to assess the spatial location of a glyph and the glyph covers only a subarea of the region it represents. The first problem may be addressed by creating thick dots at voxel midpoints, thereby generating a spatial reference that indicates the myocardial shape.

3D BEP Segments. To solve both problems, a new glyph shape has been designed that resembles a planar BEP segment extruded in 3D space (Fig. 3 (a-b)). This new shape much better fills in the region it represents. We employ three degrees of freedom: color, difference between the radius of the outer (r_{out}) and inner (r_{in}) circular arc (thickness) and height (h). The radii r_{in} and r_{out} are defined with respect to $COGmyo_s$. The segments are aligned along r_{in} which equals the average distance of myocardial voxels in s to $COGmyo_s$. The radius r_{out} of each glyph is set individually with respect to the average value of a perfusion parameter assigned to the corresponding segment. The upper limit of r_{out} is set to the maximum distance of a myocardial voxel in s to $COGmyo_s$. The angle α is set with regard to the radial position of the segment represented by the glyph. The angle β depends on the number n of segments in s and equals $360°/n$.

In Fig. 4 (c), *PE* and *Up-slope* are mapped to color and thickness. Thin bluish segments indicate a perfusion deficit. To enable a more subtle division, 40 segments have been defined by the user (10 per slice). The glyph height encodes the thickness of the original perfusion data slices. In contrast to other visualizations that interpolate between the slices pretending a comprehensive ventricular coverage, this approach conveys the considerable inter-slice gap.

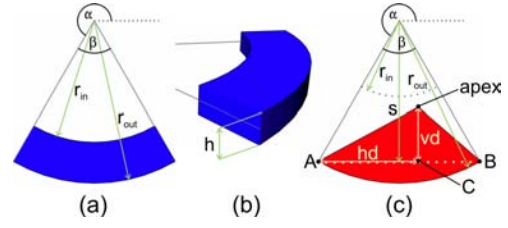**3D TIC Miniatures.** Four parameters, *PE, TTP, Integral*

Figure 3: *Construction of the 3D Bull's Eye Plot Segment (a-b) and the 3D Time-Intensity Curve Miniature (c).*

and *Up-slope*, have been approved in cardiac perfusion diagnosis (recall Sect. 2.1). However, the glyph shapes discussed above, neither allow for an integrated visualization nor for a concurrent intuitive mapping of all four parameters. Intuitive mapping here refers to the generation of an easy to learn glyph coding of TIC shape as discussed in [OMP08], e.g., by mapping *Integral* (area below the curve) to glyph size, and *Up-slope* (steepness of the ascending curve) to orientation. Hence, a new glyph shape has been designed that represents a simplified miniature of a TIC. Since physicians are trained to infer tissue characteristics from TIC shape, this glyph facilitates an easy decoding of perfusion parameters.

As can be seen in Fig. 1, *PE* and *TTP* are sufficient for constructing a triangle that resembles the TIC shape during the CA's first passage. Fig. 3 (c) illustrates the construction of the new glyph based on this observation. First, to form a visually pleasing 3D representation, the rectilinear base of the triangle (dotted line) is replaced by a circular arc. Then, the resulting shape is extruded perpendicular to its construction plane by a factor h as illustrated for the 3D BEP segments in Fig. 3 (b). While the replacement step results in a visually more pleasing representation, the construction of the glyph continuous to be based on the rectilinear base. The position of the apex relative to the base is computed as:

$$apex = C + (s - r_{in}) \times vd \times \|\overrightarrow{v}_{aux}\| \qquad (1)$$

with:

$$C = A + hd \times \|B - A\|$$
$$hd = \frac{TTPseg_{ID} - TTP_{min}}{TTP_{max} - TTP_{min}}$$
$$s = \cos(\beta/2) \times r_{out}$$
$$vd = \frac{PEseg_{ID} - PE_{min}}{PE_{max} - PE_{min}}$$

$\|\overrightarrow{v}_{aux}\| = crossProd((0,0,1)^T, \|B - A\|)$ A and B are explained in Fig. 3. The computation of hd and vd for the segment with identification *ID* is based on the corresponding averaged parameter values ($TTPseg_{ID}$ and $PEseg_{ID}$) and the

minimum and maximum for TTP and PE. The minimum of TTP (TTP_{min}) is zero and the maximum (TTP_{max}) equals the duration of the CA's first-passage. The duration is determined based on an averaged TIC in healthy tissue as the time from *CA arrival* to $Time_{End}$ (Fig. 1). For PE, both extremes (PE_{min} and PE_{max}) are simply set to the extreme values of the corresponding parameter volume. The radial orientation and extension of the glyph are defined as described for the 3D BEP segments (Fig. 3 (a)).

In Fig. 4 (d), the new triangular glyphs are presented with a coloring according to PE. The greyish glyphs, partly visible in the infarction zone, represent the averaged TIC of the entire myocardium and serve as a reference. In healthy tissue, none or just a small part of the reference TIC is visible. In contrast to the previously discussed glyphs, the new glyphs are not positioned inside the ventricle. Instead, they are pulled away from the ventricle to avoid occlusions by the scar and to provide more space for glyph construction. A pulling factor pf, which has been determined empirically so far, is multiplied with r_{in} of the glyphs: $r'_{in} = pf \times r_{in}$. The initial value of r_{in} is determined as described for the 3D BEP segments. The radius r_{out} is updated accordingly and set to a multiple of r'_{in}. The magnitude of this multiple has also been determined empirically so far.

An interesting view results from rotating the ventricle such that the view direction points down from the ventricular base along its long-axis to the apex of the ventricle (Fig. 4 (e)). The resulting view imitates a BEP and hence, gives an overview of the perfusion in all segments. This provides a reasonable default setting for an initial view when analyzing a new dataset.

Improvement of Spatial Orientation. A drawback of the visualizations discussed so far (Fig. 4 (a-e)) is a lack of spatial orientation due to the symmetry of the ventricle around its long-axis. However, physicians are used to systematically inspect the ventricle and communicate findings related to anatomical orientation cues. In 2D slices, the right ventricle serves as an orientation cue. For example, the division of the myocardium into segments and their labelling, start from the anterior connection of the left and the right ventricle. Hence, $SFrv_{LE}$ is included in the visualization as a semi-transparent surface with highlighted silhouette (Fig. 4 (f)).

Another information that is not clearly conveyed due to the transparency of $SFlv_{LE}$, is the thickness of the ventricular wall, i.e. the distance between endocardial and epicardial surface. Furthermore, if the glyphs are located outside the ventricle, such as in Fig. 4 (d), the distance between glyph and surface as well as the surface part that corresponds to a glyph, are difficult to assess. To address this problem, the intersection contours of the original perfusion data slices and $SFlv_{LE}$ are computed in 3D and emphasized by coloring them according to the corresponding glyph (Fig. 4 (f)).

Further simple techniques that support a spatial orientation are illustrated in Fig. 4 (g). An orientation cube labelled with common abbreviations for anatomical viewing directions is integrated in the lower left corner. In addition, a textured plane may be integrated which, e.g., shows a slice view of the original perfusion data. The user can interactively browse through the slices as well as trough the timepoints of a single slice, thereby examining the perfusion parameters in the anatomical context. To support the identification of a glyph and a segment, respectively, and to simplify the correlation with a BEP, each glyph may be labelled with its unique segment number. In Fig. 4 (g), the myocardium has been divided according to the AHA model. The corresponding BEP is presented in the inlet.

6. Enhancement with Contractility and Viability Information

To facilitate a joint inspection of myocardial perfusion, contractility and viability, we enhance the glyph-based visualization of perfusion parameters by integrating the parameters WT and TM (recall Subsec. 2.2).

6.1. Perfusion and Viability

Since the coronaries are attached to the epicardium, a perfusion deficit due to a decreased blood supply first appears along the endocardial wall. Therefore, also scarred tissue mostly adjoins the endocardium and TM may be measured indirectly by computing the minimum distance from the scar to the epicardium. A short distance then corresponds to a high TM. In order to assess TM, the distance from each vertex of $SFscar_{LE}$ to $SFepi_{LE}$ is computed and stored in a field associated to the vertex. The distances are then color-coded on $SFscar_{LE}$. As an example, TM has been determined and visualized for $case_1$ in Fig. 4 (h). The transmurality in this particular example is quite low over the entire scar (greenish regions). Only close to the right ventricle and at the basis, small distance values indicating a higher transmurality are revealed (dark regions). The small values at the basis can be neglected since $SFscar_{LE}$ and $SFepi_{LE}$ overlap in this region. The overlapping results from the surface generation algorithm (recall Subsec. 4.2) that produces closed surfaces and caps the epicardium and the scar in the first and last slice of their occurrence. In a more advanced solution, the caps should be removed before distance computation. We decided to keep them here for illustrating the previous discussion.

6.2. Perfusion, Contractility and Viability

The parameter WT is retrieved based on three passes of minimum distance computations. Before the distances are computed, the caps of $SFendo_{cineED}$, $SFepi_{cineED}$, $SFendo_{cineES}$ and $SFepi_{cineES}$ are removed to avoid invalid computations. In a first pass, the distances between $SFendo_{cineED}$ and $SFepi_{cineED}$ are computed and stored in fields associated to the vertices of $SFendo_{cineED}$. Next, the process is repeated for $SFendo_{cineES}$ and $SFepi_{cineES}$. After that, the wall thickness has been computed at ED and ES and is stored with

the endocardial surfaces. The latter has been chosen to allow for an occlusion-free integration of the viability information later on. In the last pass, a copy of $SFendo_{cineED}$ is generated ($SFendo'_{cineED}$) and for each vertex in this copy, the closest vertex in $SFendo_{cineES}$ is determined. Based on the field values FV_{ED} and FV_{ES} of a vertex pair, WT is calculated such that it describes the percentage increase of wall thickness from ED to ES:

$$WT[\%] = \frac{FV_{ES} - FV_{ED}}{FV_{ED}} \times 100 \qquad (2)$$

The field values of the vertices in $SFendo'_{cineED}$ are replaced by the computed WT values.

As an example, WT has been determined and visualized for $case_2$ by coloring $SFendo'_{cineED}$ according to the vertex' field values (Fig. 4 (i)). With the applied CLUT, small values are mapped to red, values around 100% to green and very high values to blue. The interpolation in between is carried out in the perceptually oriented HSV color space. Before discussing the visualization in more detail, we explain how TM has been added to this exemplary representation.

In first experiments, TM was color-coded on $SFscar_{LE}$ as in Fig. 4 (h). This of course would lead to an undesired occlusion of WT in the infarction zone. Though increasing the transparency of $SFscar_{LE}$ would reveal the occluded $SFendo'_{cineED}$, color blending would mislead the viewer. To solve the occlusion problem, we compute 3D isolines on $SFscar_{LE}$ by considering the stored distances to $SFepi_{LE}$. We superimpose the isolines on a highly transparent, colorless version of $SFscar_{LE}$ (Fig. 4 (i)). The number of isolines has been chosen empirically so far and the corresponding isovalues are uniformly distributed in the range of measured distances. While all previously discussed visualization techniques have been implemented in the software platform `MeVisLab` (MeVis Research, Bremen), the isolines were generated using `AMIRA` (Visage Imaging GmbH, Berlin).

The compact visualization of perfusion, contractility and viability in Fig. 4 (i), facilitates a joint assessment of all three aspects. In the region of the scar, the perfusion is hampered as indicated by flat bluish TICs revealing parts of their reference TICs. The red regions of the endocardium imply a loss of contractility which may be expected in the infarction zone. Close to the base, a region with a decreased WT appears that does not belong to the infarction zone which might be a hint on hibernating myocardium. The perfusion in this region cannot be assessed since the perfusion scan did not cover the top basal part. However, an assessment would be necessary within the first ≈ 2 weeks after an infarction to differentiate between stunned and hibernating myocardium. The overall transmurality of the scar is high as indicated by dark isolines (small distance values) enclosing large surface parts. Unfortunately, this must be interpreted as a negative prediction for long-term improvement of contractility.

7. Conclusion

We presented visualization techniques for the integrated analysis of perfusion parameters as well as for the joint inspection of myocardial perfusion, contractility and viability. The visualization of perfusion parameters is based on 3D glyphs which are presented in the context of anatomical data. For a voxel-wise analysis, cubes outperform other simple primitives since they optimally cover the space they represent. To solve spatial orientation problems in a segment-wise analysis and to provide a good spatial coverage of myocardial segments by the corresponding glyphs, we introduced advanced glyph types, namely the 3D BEP segment and the 3D TIC miniature. 3D BEP segments are inspired by the well established BEP. The 3D TIC miniatures provide a concurrent, intuitive mapping of all important parameters in cardiac diagnosis. They exploit the familiarity of physicists with TIC shapes. A drawback of the TIC miniatures is their variation in shape depending on the number of segments per slice. For a small number (< 6) they are considerably stretched and flattened. A further problem is that the declining part of the glyph suggests a signal decrease back to the level of *CA arrival* (see Fig. 1) which is not a valid assumption and in fact, the scanning duration is often too short to cover the entire wash-out. For the joint inspection of perfusion, contractility and viability, we suggest to combine the glyphs with a color encoding of wall thickening on the endocardial surface extracted from the cine data and isolines depicting the transmurality along the scar's surface. We applied our approach to three datasets from a clinical study. The perfusion analysis results could be validated by means of the study report.

In our future work, we plan to integrate already computed segmentation results of hypoperfused regions and a visualization of the coronary arteries. The transmurality and the wall thickening have been computed based on measuring surface distances. The effect of previously smoothing the surfaces should be further studied. A thorough evaluation, in particular, a comparison of different visualization options, with respect to clarity, comprehensibility and effectiveness of the developed techniques is open for future work.

8. Acknowledgements

References

[ASGBea01] AL-SAADI N., GROSS M., BORNSTEDT A., ET AL.: Comparison of Various Parameters for Determining an Index of Myocardial Perfusion Reserve in Detecting Coronary Stenosis with Cardiovascular Magnetic Resonance Tomography. *Z Kardiol 90*, 11 (Nov 2001), 824–34.

[ASHea99] ARHEDEN H., SAEED M., HIGGINS C. B., ET AL.: Measurement of the Distribution Volume of Gadopentetate Dimeglumine at Echo-planar MR Imaging to Quantify Myocardial Infarction: Comparison with 99mTc-DTPA Autoradiography in Rats. *Radiology 211*, 3 (1999), 698–708.

[BBP07] BLAAS J., BOTHA C., POST F.: Interactive Visualization of Multi-field Data Using Dynamically Linked Physical and Feature Space Views. In *Proc. of EuroVis* (2007), pp. 123–130.

[BPNea03] BREEUWER M., PAETSCH I., NAGEL E., ET AL.: The Detection of Normal, Ischemic and Infarcted Myocardial Tissue using MRI. In *Proc. of CARS* (2003), vol. 1256 (ICS), pp. 1153–1158.

[CKGea01] CHOI K., KIM R., GUBERNIKOFF G., ET AL.: Transmural Extent of Acute Myocardial Infarction Predicts Long-Term Improvement in Contractile Function. *Circulation 104*, 10 (2001), 1101–1107.

[CLYK03] CHOI S.-M., LEE D.-S., YOO S.-J., KIM M.-H.: Interactive Visualization of Diagnostic Data from Cardiac Images Using 3D Glyphs. In *Proc. of ISMDA* (2003), pp. 83–90.

[CWDea02] CERQUEIRA M., WEISSMAN N., DILSIZIAN V., ET AL.: Standardized Myocardial Segmentation and Nomenclature for Tomographic Imaging of the Heart. *Circulation 105*, 4 (2002), 539–542.

[HBKea07] HENNEMUTH A., BEHRENS S., KUEHNEL C., ET AL.: Novel Methods for Parameter Based Analysis of Myocardial Tissue in MR-Images. In *Proc. of SPIE Conference on Medical Image Computing* (2007), vol. 6511, pp. 65111N–1–65111N–9.

[HSB06] HUNOLD P., SCHLOSSER T., BARKHAUSEN J.: Magnetic Resonance Cardiac Perfusion Imaging - a Clinical Perspective. *European Radiology 16*, 8 (2006), 1779–1788.

[HSFea08] HENNEMUTH A., SEEGER A., FRIMAN O., ET AL.: Automatic Detection and Quantification of Non-Viable Myocardium in Late Enhancement Images. In *Proc. of ISMRM* (2008).

[LC87] LORENSEN W. E., CLINE H. E.: Marching Cubes: A High Resolution 3D Surface Construction Algorithm. In *Proc. of SIGGRAPH* (1987), pp. 163–169.

[NHBR04] NOBLE N., HILL D., BREEUWER M., RAZAVI R.: The Automatic Identification of Hibernating Myocardium. In *Proc. of MICCAI* (2004), pp. 890–898.

[NM65] NELDER J., MEAD R.: A Simplex Method for Function Minimization. *Computer Journal 7*, 4 (1965), 308–313.

[ODHea07] OELTZE S., DOLEISCH H., HAUSER H., ET AL.: Interactive Visual Analysis of Perfusion Data. *IEEE Trans. Vis. Comput. Graph. 13*, 6 (2007), 1392–1399.

[OGHea06] OELTZE S., GROTHUES F., HENNEMUTH A., ET AL.: Integrated Visualization of Morphologic and Perfusion Data for the Analysis of Coronary Artery Disease. In *Proc. of EUROVIS* (2006), pp. 131–138.

[OMP08] OELTZE S., MALYSZCZYK A., PREIM B.: Intuitive Mapping of Perfusion Parameters to Glyph Shape. In *Proc. of BVM* (2008), pp. 262–266.

[PGYea01] PANTING J., GATEHOUSE P., YANG G., ET AL.: Echo-planar Magnetic Resonance Myocardial Perfusion Imaging: Parametric Map Analysis and Comparison with Thallium SPECT. *J Magn Reson Imaging 13*, 2 (2001), 192–200.

[POHea07] PAASCHE L., OELTZE S., HENNEMUTH A., ET AL.: Integrierte Visualisierung kardialer MR-Daten zur Beurteilung von Funktion, Perfusion und Vitalität des Myokards. In *Proc. of BVM* (2007), pp. 212–216.

[RMSSea07] ROPINSKI T., MEYER-SPRADOW J., SPECHT M., ET AL.: Surface Glyphs for Visualizing Multimodal Volume Data. In *Proc. of VMV* (2007), pp. 3–12.

[RP08] ROPINSKI T., PREIM B.: Taxonomy and Usage Guidelines for Glyph-based Medical Visualization. In *Proc. of SimVis* (2008), pp. 121–138.

[SBDea86] SHEEHAN F., BOLSON E., DODGE H., ET AL.: Advantages and Applications of the Centerline Method for Characterizing Regional Ventricular Function. *Circulation 74*, 2 (1986), 293–305.

[SPP00] SCHENK A., PRAUSE G., PEITGEN H.-O.: Efficient Semiautomatic Segmentation of 3D Objects in Medical Images. In *Proc. of MICCAI* (2000), pp. 186–195.

[SRFN06] SELVANAYAGAM J., ROBSON M., FRANCIS J., NEUBAUER S.: Cardiovascular Magnetic Resonance: Basic Principles, Methods and Techniques. In *Cardiac CT, PET and MR*, Dilsizian V., Pohost G., (Eds.). Malden: Blackwell Publishing, 2006, pp. 28–68.

[SSJea06] SÄRING D., STORK A., JUCHHEIM S., ET AL.: HeAT: A Software Assistant for the Analysis of LV Remodeling after Myocardial Infarction in 4D MR Follow-Up Studies. In *Proc. of GI Jahrestagung (1)* (2006), pp. 537–543.

[Tau95] TAUBIN G.: A Signal Processing Approach to Fair Surface Design. In *Proc. of SIGGRAPH* (1995), pp. 351–358.

[TBBea07] TERMEER M., BESCÓS J., BREEUWER M., ET AL.: CoViCAD: Comprehensive Visualization of Coronary Artery Disease. *IEEE Trans. Vis. Comput. Graph. 13*, 6 (2007), 1632–1639.

[WLY04] WÜNSCHE B. C., LOBB R., YOUNG A. A.: The Visualization of Myocardial Strain for the Improved Analysis of Cardiac Mechanics. In *Proc. of GRAPHITE* (2004), pp. 90–99.
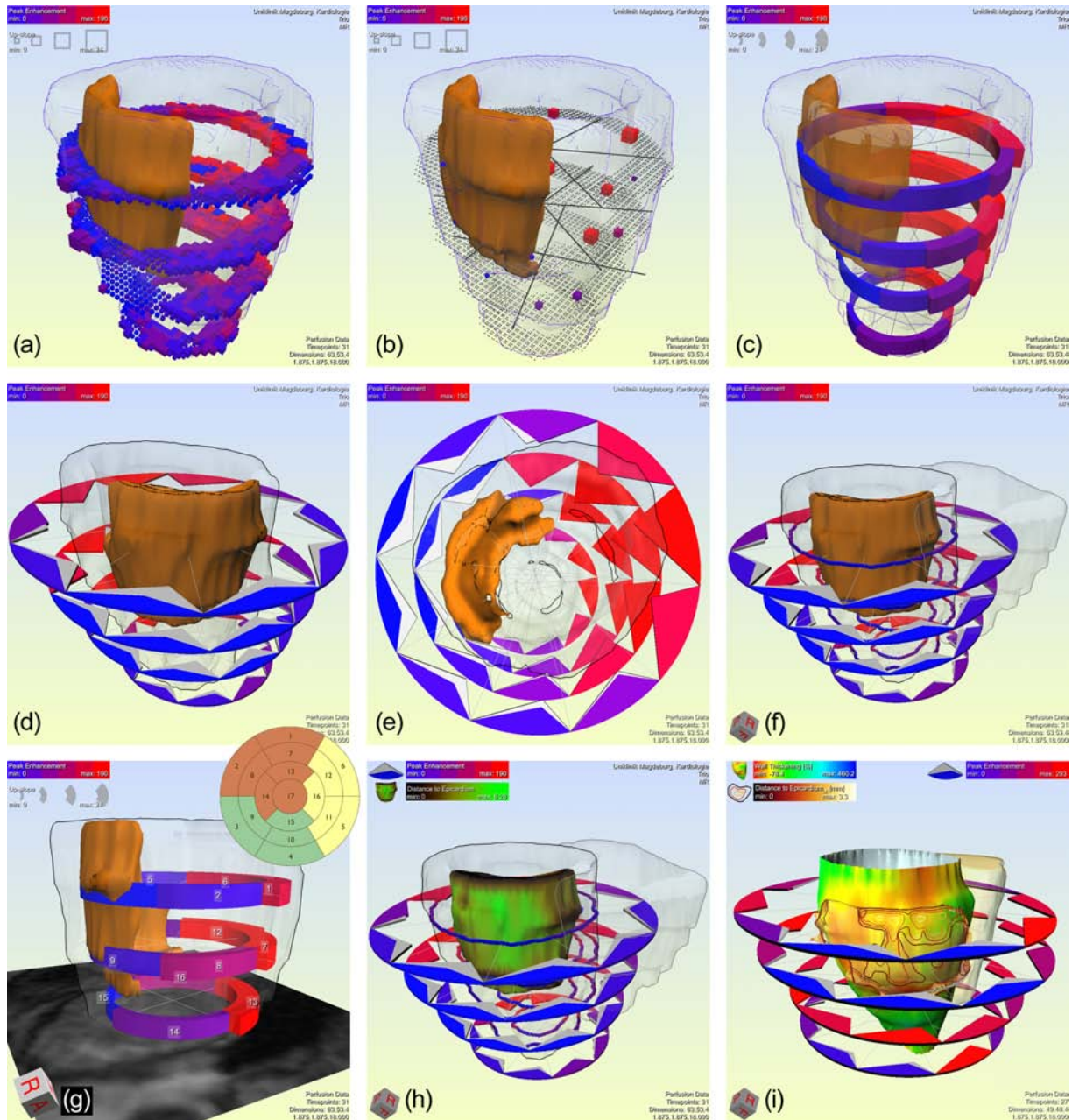
Figure 4: *Glyph-based visualization of myocardial perfusion and enhancement with contractility and viability information. In each sub-image, the glyph color encodes PE. In* (a-h)*, the left ventricle is rendered semi-transparently and the infarction scar as colored surface inside the ventricular wall.* (a) *Cubes encoding Up-slope (size) and PE are placed voxel-wise.* (b) *Cubes are placed segment-wise (AHA model). Segment borders are represented by lines and dots are drawn at myocardial voxels.* (c) *A user-defined segment-wise analysis by means of 3D BEP segments. The glyph height corresponds to the thickness of the perfusion slices, while the glyph thickness encodes Up-slope.* (d) *For each segment, a 3D TIC miniature resembles the averaged TIC shape. The TIC of the entire myocardium is superimposed (grey glyphs).* (e) *The view along the ventricular long-axis resembles a BEP view.* (f) *The right ventricle is provided as context information. The left ventricular wall is emphasized at intersections with the perfusion slices.* (g) *The glyphs are labelled to indicate the correspondence with the BEP (inlet).* (h) *The scar's color encodes its distance to the epicardium. Dark parts exhibit a high transmurality.* (i) *The wall thickening is color-coded on the endocardium. Red regions exhibit a decreased contractility. Isolines encode the scar's distance to the epicardium. Its overall transmurality is high, indicated by dark isolines (small distance values) enclosing large surface parts.*